ELSEVIER

Polymer 43 (2002) 1307–1311

polymer

www.elsevier.com/locate/polymer

A kinetic analysis on the gas phase polymerization of ethylene over polymer supported $(CH_3)_2Si[Ind]_2ZrCl_2$ catalyst

J.S. Chung, J.C. Hsu*

Department of Chemical Engineering, Queen's University, Kingston, Ont., Canada K7L3N6

Received 31 May 2001; received in revised form 15 October 2001; accepted 19 October 2001

Abstract

Kinetics of the gas phase polymerization of ethylene over polymer supported $(CH_3)_2Si[Ind]_2ZrCl_2$ catalyst is examined. It requires a two-site model to adequately describe the experimental results. The active sites seem to follow a first-order deactivation. The number of sites activated is dependent upon the cocatalyst (MAO) concentration level as well as temperature. It was observed that the decrease of activity at higher temperatures resulted from a strong dependency of the first-order decay rate constant on temperature. On the other hand, the propagation rate constants of two active sites show similar dependency on temperature. © 2001 Elsevier Science Ltd. All rights reserved.

Keywords: Polymer supported; Metallocene; Gas phase ethylene polymerization

1. Introduction

The discovery of homogeneous metallocene catalysts in the early 1980s opened a new era for olefin polymerization. These metallocene catalyst systems are basically homogeneous. However, in order for the metallocene catalysts to be used in the prevailing slurry or gas phase processes, the catalysts must be supported on a solid. In addition, since most existing commercial polymerization processes that involve Ziegler–Natta catalysts are heterogeneous in nature, to convert these processes for employing metallocene catalysts it is necessary that the metallocene catalysts should also be in a heterogeneous state. In recent papers [1–3], a variety of supports such as SiO_2 and Al_2O_3 have been reported, but there are other possibilities of interests, such as the use of a polymer as support.

Metallocene catalysts have the advantages of high activity and of producing polymer with special properties. One of the distinguished properties is narrow molecular weight distribution (MWD, M_w/M_n) of polymer product. The advantage of using polymer as support is the lowering of inorganic residues in the final product. Furthermore, manipulating the functional groups in polymer support opens the possibility of controlling the molecular structure of polymer. In this study, we will discuss the results of a kinetic analysis on the polymer supported $(CH_3)_2Si[Ind]_2ZrCl_2$ catalyst (MEZ) for ethylene gas phase polymerization.

2. Experimental

The experimental work was done by Tairova et al. [4]. Here a brief description of the experimental procedure is given.

2.1. Preparation of polymer support and polymer-supported catalysts

In the preparation of support, 10 g of 2% cross-linked chloromethylated styrene/divinylbenzene were mixed with 100 ml of dichlorobenzene, 3 ml of 40% tetrabutylammonium hydroxide, 30 g of potassium acetate, 20 g of KOH and 60 ml of deionized water. After the mixture was stirred for 3 days at 85 °C, the polymer was filtered and washed by water, methanol, THF/water (3:1), THF, water, acetone, and finally dichloromethane. The solids were dried completely in vacuum at 85 °C. The resulting polymer support was analyzed by IR, which showed a complete disappearance of the absorption peak of chloromethylated benzene at 1264 cm^{-1}.

In preparing the supported catalysts, the hydroxylated polymer support was first treated with 36 mmol of MAO in the presence of toluene and 200 ml of heptane at 50 °C for 20 h. During the reaction, it was observed that a small amount of gas was evolved, indicating the reaction of MAO

* Corresponding author. Tel.: +1-613-533-2786; fax: +1-613-533-6637.
E-mail address: hsuc@chee.queensu.ca (J.C. Hsu).

PII: S0032-3861(01)00716-9

Table 1
Summary of ethylene polymerization experiments with polymer supported $(CH_3)_2Si[Ind]_2ZrCl_2$ catalyst [4]

Run no.	Temperature (°C)	C_2H_4 pressure (atm)	MAO level (mmol)	Activity (kgPE/g-Zr/atm/h)
1	60	4	2.5	11.3
2	80	4	2.5	26.1
3	60	4	10	8.3
4	80	4	10	41.7
5	60	2	5	25.8
6	80	2	5	32.0
7	60	6	5	5.0
8	80	6	5	20.4
9	70	2	2.5	9.6
10	70	2	10	23.0
11	70	6	2.5	11.4
12	70	6	10	23.6
13	70	4	5	24.6
14	70	4	5	25.7
15	70	4	5	21.2

with OH groups in the support. The solids after reaction were filtered, washed with 100 ml toluene, and dried at room temperature under vacuum. 300 mg of zirconocene catalyst in 250 ml of toluene were then added to the support at 40 °C and let them react for 6–10 h in toluene. The catalyst was then filtered, washed with 100 ml toluene, and dried at room temperature under vacuum. The average zirconium content in the catalyst was found to be 0.17% by weight.

2.2. Polymerization

A horizontal stirred-bed reactor (10.2 cm diameter × 10.2 cm length), made of stainless steel, was used for the gas-phase polymerization. The reactor was operated in a semi-batch mode. The mixer contains three Teflon blades attached to a shaft that rotates at 300 rpm. Temperature control to within ±0.5 °C was accomplished by circulating a coolant to an internal cooling coil with heating from outside by an electrical heating tape.

Table salt was used as seed bed. The catalyst was activated outside the reactor by mixing catalyst and cocatalyst with a small amount of toluene. After injecting into the reactor, the reactor was evacuated to remove solvent. The reactor was then pressurized quickly with ethylene. By maintaining a constant pressure in the reactor, the polymerization rate was measured as the flow rate of monomer to the reactor and recorded on a personal computer. The polymerization was carried out according to Box–Behnken experimental design [5] for three factors—temperature, ethylene partial pressure and MAO level. A total of 15 experiments were carried out, and the experimental conditions and their results are given in Table 1. The molar ratio of MAO to zirconium ranged from 2683 to 10,731.

3. Model development

It is well known that homogeneous metallocene catalysts contain a uniform active site. However, if they are immobilized on a support, the MWD of the polymer produced from the supported catalyst becomes broader comparing with a homogeneous system [4,6]. A few papers have reported that immobilization of metallocene catalysts could result in diversifying the characteristics of active sites [6]. With respect to the catalyst deactivation it has been reported that silica supported MEZ/MAO catalysts show a first order deactivation in the gas phase ethylene polymerization [7]. However, our catalyst is polymer supported and is heterogeneous in nature. The catalytic activity may behave differently.

For this reason, four different models, single-site first-order deactivation, single-site second-order deactivation, dual-site first-order deactivation and dual-site second-order deactivation were used to fit 15 experimental results individually to examine which model would give the best result. The assumption of two types of sites, one being highly active with fast deactivation (site A) and one being less active with slow deactivation (site B) was originated from the earlier studies on the heterogeneous Ziegler–Natta catalyst systems [8,9].

However, the estimated kinetic parameters obtained from each experiment do not provide a meaningful value, since the kinetic parameters are function of polymerization conditions such as temperature, monomer concentration and cocatalyst concentration, which are different for each experiment. A single model was then used to describe this functional relationship.

For the catalyst containing two active sites, the rate equation can be written as,

$$R_p = [M]\sum_{i=1}^{2} k_{p,i} C_i^* \tag{1}$$

where R_p is the rate of polymerization in g-PE g-cat^{-1} h^{-1}, $[M]$ is the monomer concentration in g m^{-3}, $k_{p,i}$ is the propagation rate constant in m^3 mol^{-1} h^{-1} for i-site, and C_i^* is the concentration of active sites in mol g-cat^{-1} for i-site. If the

Table 2
Results of averaged standard deviation over 15 experiments

	Residual standard deviation[a]	Relative standard deviation[b]
First-order single-site	24.62	0.142
First-order dual-site	7.43	0.0618
Second-order single-site	21.57	0.1047
Second-order dual-site	8.97	0.0766

[a] Defined as $\sqrt{\sum_{i=1}^{n}((Y'(i)-Y(i))^2/(n-2)}$, $Y'(i)$ = experimental rate value, $Y(i)$ = calculated rate value, n = number of observation.

[b] Defined as $\sqrt{\sum_{i=1}^{n}[(2(Y'(i)-Y(i))/(Y'(i)+Y(i))]^2/(n-2)}$.

active site of the catalyst is deactivated according to first-order decay, the rate equation becomes,

$$R_p = [M]\sum_{i=1}^{2} k_{p,i}C^*_{0,i}\exp(-k'_{d,i}t) \tag{2}$$

where $C^*_{0,i}$ is the initial concentration of active sites for i-site, $k'_{d,i}$ is the first-order catalyst decay constant in 1 h^{-1}, and t is the polymerization time in hours. For a second-order decay the equation becomes

$$R_p = [M]\sum_{i=1}^{2} k_{p,i}C^*_{0,i}/(1 + k''_{d,i}C^*_{0,i}t) \tag{3}$$

where $k''_{d,i}$ is the second-order catalyst decay constant in g-cat mol^{-1} h^{-1}. In our previous study [4], we found that the catalyst activity could be correlated using a quadratic form with a second-order effect of MAO and an interaction effect of MAO with temperature. It can be written as,

$$C^*_{0,i} = C^{**}_{0,i}(a + b[\mathrm{MAO}]T + c[\mathrm{MAO}]^2) \tag{4}$$

where $C^{**}_{0,i}$, a, b, and c are correlation coefficients. Based on this assumption, Eqs. (2) and (3) can be modified as follows,

$$R_p = [M]\sum_{i=1}^{2} k_{p,i}C^{**}_{0,i}(a + b[\mathrm{MAO}]T + c[\mathrm{MAO}]^2)\exp(-k'_{d,i}t) \tag{5}$$

or

$$R_p = [M]\sum_{i=1}^{2} k_{p,i}C^{**}_{0,i}a(1 + b/a[\mathrm{MAO}]T + c/a[\mathrm{MAO}]^2)\exp(-k'_{d,i}t) \tag{6}$$

and

$$R_p = [M]\sum_{i=1}^{2} k_{p,i}C^{**}_{0,i}a(1 + b/a[\mathrm{MAO}]T + c/a[\mathrm{MAO}]^2)/\{1 + k''_{d,i}C^{**}_{0,i}a(1 + b/a[\mathrm{MAO}]T + c/a[\mathrm{MAO}]^2)t\} \tag{7}$$

$k_{p,i}$, $k'_{d,i}$, and $k''_{d,i}$ in Eqs. (6) and (7) are functions of temperature, defined as,

$$k_{p,i} = k_{p0,i}\exp(-E_{p,i}/RT) \tag{8}$$

$$k'_{d,i} = k'_{d0,i}\exp(-E'_{d,i}/RT) \tag{9}$$

$$k''_{d,i} = k''_{d0,i}\exp(-E''_{d,i}/RT) \tag{10}$$

where $k_{p0,i}$, $k'_{d0,i}$, and $k''_{d0,i}$ are pre-exponential terms, $E_{p,i}$, $E'_{d,i}$, and $E''_{d,i}$ are corresponding activation energies, R is gas constant, and T is temperature in K.

Eqs. (6) and (7) were applied to all data set shown in Table 1 excluding Run 6, where the catalyst showed no deactivation, a surprising observation that might be due to experimental error. With these models, kinetic parameters for the polymer supported MEZ catalyst for gas-phase ethylene polymerization were estimated. Optimization routine was carried out using Fletcher–Reeves–Polak–Ribiere minimization method [10]. Initial conditions were chosen over a broad range of their values to avoid approaching local minimum. The range of initial conditions was determined by the physical meaning of each parameter. For example, $E_{p,1}$ was generally reported in the range of 7–15 kcal mol^{-1}; a range of 5–20 kcal mol^{-1} was chosen. Once the initial range was decided, it was divided into 10–100 grids to search for the minimum for more sensitive parameters. For less sensitive parameters a grid of 10 or less was used. Constraints, such as $ak_{p0,1}C^{**}_{0,1} > ak_{p0,2}C^{**}_{0,2}$, $E_{p,1} < E_{p,2}$, and $k'_{d0,1} > k'_{d0,2}$ were also applied. Statistical results from the fitting are given in Table 2.

4. Results and discussion

The standard deviations between the experimental observations and the estimated values were calculated for each run. The residual standard deviations and relative standard deviations averaged over the 14 experiments are given in Table 2. From those results and also from Fig. 1 and Table 2, we can see that the dual-site first-order deactivation model is the best fitted model even though the difference between the first-order model and the second-order model is quite small.

Fig. 2 shows a typical comparison between experiment and model profiles. The overall correlation coefficient was 0.956, which means a reasonable fit of the model to the

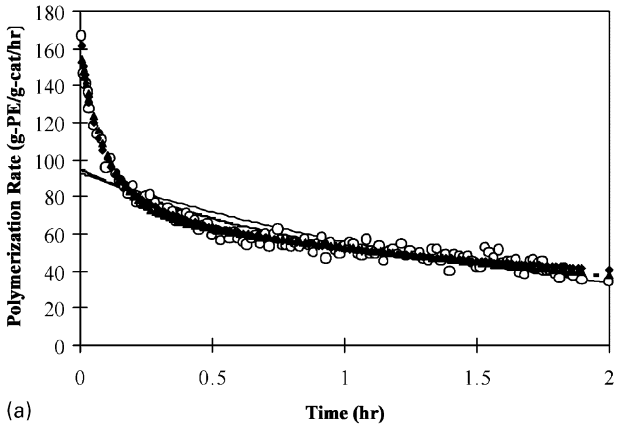

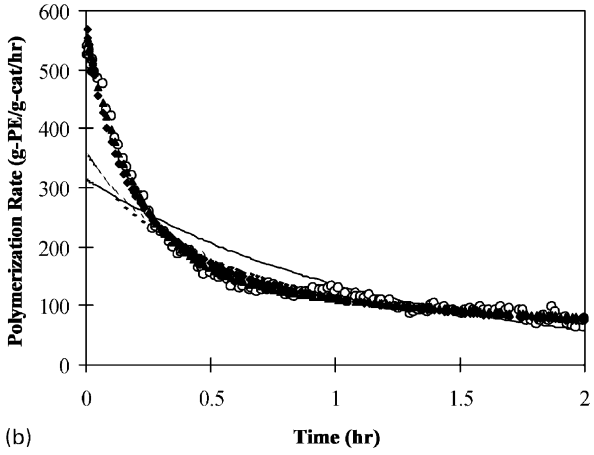

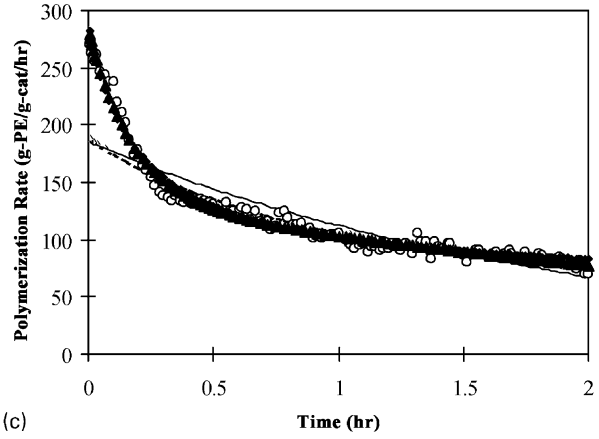

Fig. 1. (a) Experimental and model calculated rate profiles of ethylene polymerization. For Run 1: experimental (○); single-site first-order decay (- - -); single-site second-order decay (—); dual-site first-order decay (▲); dual-site second-order decay (◆). (b) Experimental and model calculated rate profiles of ethylene polymerization. For Run 8: experimental (○); single-site first-order decay (- - -); single-site second-order decay (—); dual-site first-order decay (▲); dual-site second-order decay (◆). (c) Experimental and model calculated rate profiles of ethylene polymerization. For Run 13: experimental (○); single-site first-order decay (- - -); single-site second-order decay (—); dual-site first-order decay (▲); dual-site second-order decay (◆).

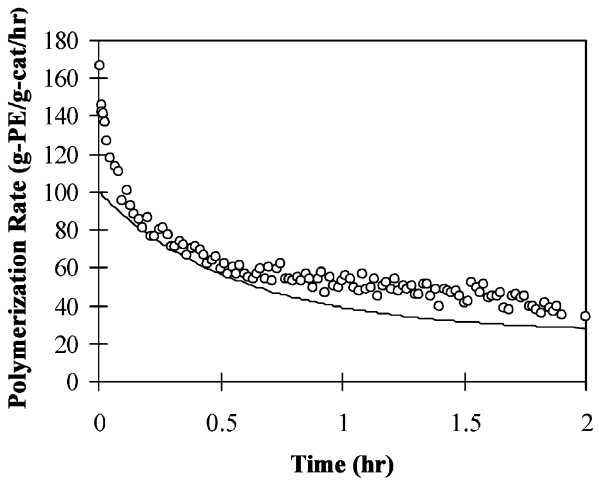

Fig. 2. Typical experimental and model calculated rate profiles of ethylene. Polymerization over polymer-supported MEZ catalyst (Run 1): experimental (○); model calculated (—).

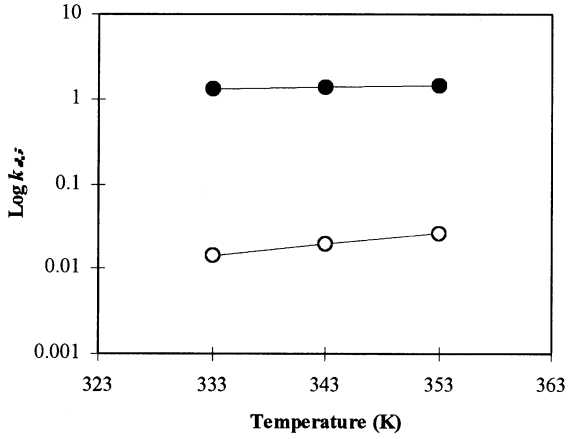

Fig. 3. Variation of $k_{d,i}$ with respect to the reaction temperature: (●) site A; (○) site B.

Table 3
Results of estimated kinetic parameters

Kinetic parameter	Units	Estimated value
$ak_{p0,1}C^{**}_{0,1}$	m^3 g-cat^{-1} h^{-1}	95927.9
$E_{p,1}$	kcal mol^{-1}	10.454
$k'_{d0,1}$	1 h^{-1}	45.32
$E'_{d,1}$	kcal mol^{-1}	2.114
$ak_{p0,2}C^{**}_{0,2}$	m^3 g-cat^{-1} h^{-1}	86135.9
E_{p2}	kcal mol^{-1}	10.94
$k'_{d0,2}$	1 h^{-1}	741.70
$E'_{d,2}$	kcal mol^{-1}	6.152
b/a	1 mol^{-1} K^{-1}	0.352
c/a	1 mol^{-2}	0.000011

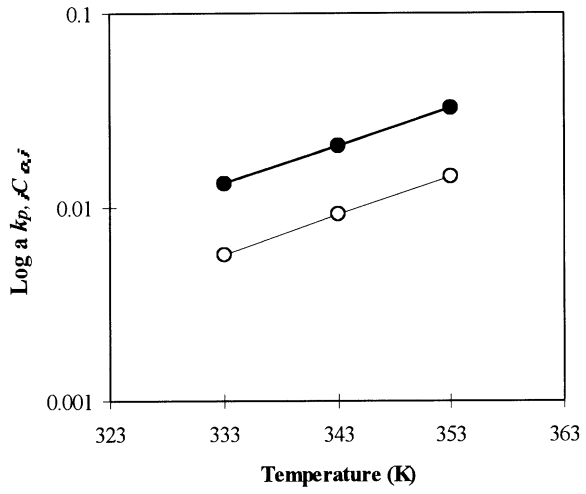

Fig. 4. Variation of $k_{p,i}$ with respect to the reaction temperature: (●) site A; (○) site B.

experimental results. A perfect fit was not obtained, particularly at the initial stage of polymerization. This lack of fit at the initial stage of polymerization should not deter our analysis on the kinetic parameters.

As shown in Table 3, the estimated parameters show the characteristics of each site clearly. The estimated activation energies for the propagation rates of the two active sites were very close to each other. On the other hand, significant difference was observed in activation energies for deactivation of two active sites. The activation energy for deactivation reaction of site B is three times larger than that of site A. As a result, $k'_{d,B}$ of site B is greatly affected by the temperature. Fig. 3 also shows that $k'_{d,A}$ of site A is hardly changed with temperature. And as shown in Fig. 4, k_p's of the two active sites have similar slopes with respect to temperature. It can then be concluded that it is most likely that site B is mainly responsible for the decrease in activity at higher temperatures.

Acknowledgements

We acknowledge the financial support from the National Sciences and Engineering Research Council of Canada and Seoam Scholarship Foundation in Korea.

References

[1] Soga K, Kaminaka M. Macromol Chem Rapid Commun 1992;13:221–4.
[2] Soga K, Kaminaka M. Macromol Chem Phys 1994;195:1369–77.
[3] Hlatky GG. Chem Rev 2000;100:1347–76.
[4] Tairova G, Zhang Y, McAuley KB, Bacon DW. Development of polymer supported metallocene catalysts for gas phase olefin polymerization. Final Report to ESTAC, 1999.
[5] Box GEP, Wilson KP. J Roy Stat Soc 1951;b13:1–13.
[6] Kim JD, Soares BP, Rempel GL. J Polym Sci Part A: Polym Chem 1999;37:331–9.
[7] Roos P, Meier GB, Samson JJC, Weickert G, Westerterp KR. Macromol Rapid Commun 1997;18:319–24.
[8] Dumas C, Hsu CC. J Appl Polym Sci 1989;37:1625–44.
[9] Tait PTT, Wang S. Br Polym J 1988;20:499–508.
[10] Press WH, Teukolsky SA, Vetterling WT, Flannery BP. Numerical recipes in C. 2nd ed. Cambridge: Cambridge University Press, 1992. Chapter 10.